

Quantum Unidirectional Magnetoresistance

M. Mehraeen, Pengtao Shen, and Steven S.-L. Zhang*

Department of Physics, Case Western Reserve University, Cleveland, OH 44106, USA

(Dated: September 1, 2021)

We predict a unidirectional magnetoresistance effect arising in a bilayer composed of a nonmagnetic metal and a ferromagnetic insulator, whereby both longitudinal and transverse resistances vary when the direction of the applied electric field is reversed or the magnetization of the ferromagnetic layer is rotated. In the presence of spin-orbit coupling, an electron wave incident on the interface of the bilayer undergoes a spin rotation and a momentum-dependent phase shift. Quantum interference between the incident and reflected waves furnishes the electron with an additional velocity that is even in the in-plane component of the electron's wavevector, giving rise to the unidirectional magnetoresistance – a nonlinear magnetotransport effect that is rooted in the wave nature of electrons.

Introduction.—As fingerprints of electron waves, quantum interference effects in electron transport have been of fundamental interest [1–7]. And from the perspective of applications, studies of coherent quantum transport of electrons – and more generally information carriers – may also underpin the development of future quantum devices, including quantum computers [8].

Notable examples of interference-based electron transport include the weak localization (WL) and weak antilocalization (WAL) effects [2, 3], with distinctive magnetotransport signatures [9, 10]: a negative magnetoresistance arising from WL and a positive one from WAL. Both types of magnetoresistances emerge in the *linear* response regime and stay *invariant* under the reversal of the applied magnetic field.

Recently, there has been increasing interest in an emergent unidirectional magnetoresistance (UMR) effect observed in various bilayer systems composed of a nonmagnetic layer and a ferromagnetic layer [11–15]. This novel nonlinear magnetotransport effect features a variation in magnetoresistance when the direction of the applied electric field is reversed, at variance with common linear magnetoresistances – like the ones due to WL and WAL – that are electric-field independent.

While the list of systems that can host such UMRs keeps growing, they consistently possess three essential ingredients: strong spin-orbit coupling (SOC), structural inversion asymmetry, and broken time reversal symmetry. In terms of microscopic mechanisms, lying at the heart of UMR effects are the spin-momentum coupling and spin-asymmetry in electron scattering [13, 15–18]. Quantum interference, however, has not been demonstrated to play any role in nonlinear magnetotransport.

In this work, we unveil the role of quantum interference in generating both *longitudinal* and *transverse* UMRs in bilayer structures consisting of a nonmagnetic metal (NM) and a ferromagnetic-insulator (FI), in the presence

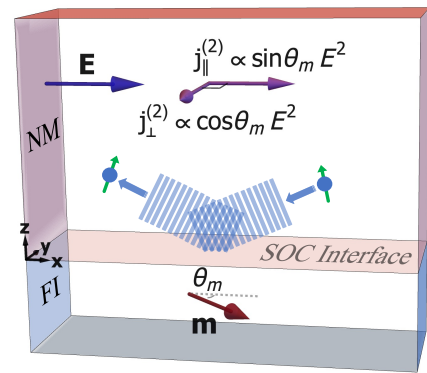


FIG. 1. Schematic of the quantum unidirectional magnetoresistance (QUMR) effect in a NM|FI bilayer. An electron in the NM layer scatters off the interface with spin-orbit coupling (SOC), resulting in an interference between the incident and reflected waves, which in turn gives rise to a nonlinear current. Both longitudinal and transverse components of the nonlinear current, $j_{\parallel}^{(2)}$ and $j_{\perp}^{(2)}$, are sensitive to the orientation of the in-plane magnetization \mathbf{m} relative to the electric field \mathbf{E} , with different dependences on θ_m – the angle between \mathbf{m} and \mathbf{E} .

of SOC at the interface. Microscopically, the scattering of an electron wave at such an interface hinges on the wavevector and spin orientations of the incident electron, as shown schematically in Fig. 1. Due to the interference between the incident and reflected waves, the electron acquires an additional velocity that is *even* in the in-plane component of the wavevector (as we will show explicitly), which in turn gives rise to a nonlinear current density of the following form:

$$\mathbf{j}^{(2)} = \sigma_{\parallel}^{(2)} \mathbf{z} \cdot (\mathbf{E} \times \mathbf{m}) \mathbf{E} + \sigma_{\perp}^{(2)} \mathbf{E} \cdot \mathbf{m} \mathbf{z} \times \mathbf{E}, \quad (1)$$

where \mathbf{E} is the applied electric field, \mathbf{m} and \mathbf{z} are two unit vectors denoting, respectively, the directions of magnetization of the ferromagnetic layer and the normal to the bilayer interface. $\sigma_{\parallel}^{(2)}$ and $\sigma_{\perp}^{(2)}$, both being \mathbf{E} -

independent, characterize, respectively, the strengths of the longitudinal and transverse contributions to the non-linear transport, with the superscripts indicating that $\mathbf{j}^{(2)}$ is of the second order in the electric field.

Given the quantum mechanical origin of the phenomena, we shall refer to the corresponding UMRs as *quantum unidirectional magnetoresistances* (QUMRs), in order to distinguish them from their semiclassical counterparts that have heretofore been reported.

The model.—For simplicity, we shall restrict ourselves to the nonlinear magnetotransport in a NM|FI bilayer, whereby electrons incident on the interface are completely reflected back into the NM layer and hence the charge transport in the ferromagnetic layer can be disregarded. Furthermore, we assume the presence of an exchange interaction – coupling the electron spin and the interfacial magnetization of the FI – and a Rashba-type SOC arising from the structural inversion asymmetry at the interface. Consider a setup described by Fig. 1, with a three-dimensional (3D) electron gas contained in a semi-infinite NM layer occupying the $z > 0$ half-space and a FI layer occupying the other half.

The 3D electron gas can be described by the Hamiltonian

$$\hat{H} = \frac{\hat{\mathbf{p}}^2}{2m_e^*} + \frac{\alpha_R}{\hbar} \delta(z) \hat{\sigma} \cdot (\hat{\mathbf{p}} \times \mathbf{z}) - J_{ex} \delta(z) \hat{\sigma} \cdot \mathbf{m} + V_b \Theta(-z), \quad (2)$$

where α_R and J_{ex} are the coefficients of the interfacial Rashba SOC and exchange interaction, respectively, and V_b is the height of the energy barrier, which is greater than the Fermi energy of electrons in the NM layer.

The general scattering state may be written as

$$\psi_{\text{scat.}} = \begin{cases} e^{i\mathbf{q} \cdot \boldsymbol{\rho}} \left(e^{-ik_z z} + e^{ik_z z} \hat{R} \right) \boldsymbol{\chi}, & z > 0 \\ e^{i\mathbf{q} \cdot \boldsymbol{\rho}} e^{\kappa z} \hat{T} \boldsymbol{\chi}, & z < 0 \end{cases}, \quad (3)$$

where $\mathbf{q} [= (k_x, k_y)]$ and $\boldsymbol{\rho} [= (x, y)]$ are the wave- and position-vector in the x - y plane, wherein the system is translationally invariant and allows the propagation of plane waves, k_z is the z -component of the wavevector of the propagating wave in the NM layer, and $\kappa^{-1} [= (2m_e^* V_b / \hbar^2 - k_z^2)^{-1/2}]$ characterizes the decay length of the evanescent wave in the FI layer. \hat{R} and \hat{T} are 2×2 matrices in spin space, which describe, respectively, the spin-dependent reflection and transmission amplitudes, and the spinors $\boldsymbol{\chi}$ are taken to be the eigenstates satisfying $\hat{\sigma} \cdot \mathbf{m} \boldsymbol{\chi}^\pm = \pm \boldsymbol{\chi}^\pm$.

By imposing the standard boundary conditions at the Rashba interface, namely the continuity of the wavefunction and the discontinuity of its spatial derivative along the z direction, we find [19]

$$\hat{R} = \frac{\mathbf{Q}_{\mathbf{q}}^2 - (\kappa^2 + k_z^2) + 2ik_z \hat{\sigma} \cdot \mathbf{Q}_{\mathbf{q}}}{(\kappa - ik_z)^2 - \mathbf{Q}_{\mathbf{q}}^2}, \quad (4)$$

and $\hat{T} = 1 + \hat{R}$. Here, $\mathbf{Q}_{\mathbf{q}} \equiv \eta_R \mathbf{q} \times \mathbf{z} - \xi_{ex} \mathbf{m}$, with $\eta_R \equiv 2m_e^* \alpha_R / \hbar^2$ a dimensionless constant characterizing the strength of the interfacial Rashba SOC and $\xi_{ex} \equiv 2m_e^* J_{ex} / \hbar^2$ the rescaled exchange interaction. Note that \hat{R} is unitary, as enforced by the conservation of probability flux.

Phase shift.—All key information about the reflected wave, such as the phase shift, in particular, is encapsulated in the matrix of the reflection amplitude. To see this, let us rewrite \hat{R} in an equivalent – but more illuminating – form as follows

$$\hat{R} = \exp(i\varphi_{\mathbf{q}}) \exp(i\vartheta_{\mathbf{q}} \hat{\sigma} \cdot \mathbf{n}_{\mathbf{q}}), \quad (5)$$

where $\varphi_{\mathbf{q}} = \arcsin(2k_z \kappa / \xi_{\mathbf{q}})$, $\vartheta_{\mathbf{q}} = \arcsin(2k_z Q_{\mathbf{q}} / \xi_{\mathbf{q}})$, with $Q_{\mathbf{q}}$ the length of the vector $\mathbf{Q}_{\mathbf{q}}$ defined above, $\xi_{\mathbf{q}}^2 = [Q_{\mathbf{q}}^2 - (\kappa^2 + k_z^2)]^2 + (2k_z Q_{\mathbf{q}})^2$, and $\mathbf{n}_{\mathbf{q}} = \mathbf{Q}_{\mathbf{q}} / Q_{\mathbf{q}}$.

Now the physical meaning of \hat{R} has become more evident: The angle $\varphi_{\mathbf{q}}$ describes a largely spin-independent phase shift, in conjunction with a spin rotation by an angle $\vartheta_{\mathbf{q}}$ about a rotation axis taken in the direction of $\mathbf{n}_{\mathbf{q}}$. Note that both $\vartheta_{\mathbf{q}}$ and $\mathbf{n}_{\mathbf{q}}$ depend, through the vector $\mathbf{Q}_{\mathbf{q}}$, on the wavevector \mathbf{q} and the magnetization \mathbf{m} , as the spin rotation is brought about by the interfacial exchange interaction and Rashba SOC.

Interference velocity.—What is relevant to the charge transport in the NM layer is the spin-averaged velocity of a conduction electron therein, which is given by the expectation value of the velocity operator with respect to the spinor part of the scattering state for $z > 0$, *i.e.*,

$$\langle \hat{v} \rangle \equiv \sum_{\sigma} \text{Re} \left[(\psi_{\text{scat.}}^{\sigma})^{\dagger} \frac{\hat{\mathbf{p}}}{m_e^*} (\psi_{\text{scat.}}^{\sigma}) \right] = \langle \hat{v} \rangle_I + \langle \hat{v} \rangle_R + \langle \hat{v} \rangle_{I-R}, \quad (6)$$

where the sum runs over the spin index. This velocity can be decomposed into three parts, as shown in Eq. (6). The first two terms, $\langle \hat{v} \rangle_I$ and $\langle \hat{v} \rangle_R$, are associated with the incident and reflected waves, respectively, and more intriguingly, there exists another term, $\langle \hat{v} \rangle_{I-R}$, originating from the interference between the incident and the reflected waves. The in-plane component of this *interference velocity* can be expressed as

$$\langle \hat{v}_{\parallel} \rangle_{I-R} = \frac{4\hbar \mathbf{q}}{m_e^*} \cos(\vartheta_{\mathbf{q}}) \cos(2k_z z + \varphi_{\mathbf{q}}), \quad (7)$$

where $\hat{v}_{\parallel} = (\hat{v}_x, \hat{v}_y)$.

There are two crucial differences between the interference velocity $\langle \hat{v} \rangle_{I-R}$ and the other counterparts, as displayed in Fig. 2. While $\langle \hat{v} \rangle_I$ and $\langle \hat{v} \rangle_R$ share the same in-plane component $\frac{\hbar \mathbf{q}}{m_e^*}$ (which is clearly odd in \mathbf{q}), the interference velocity $\langle \hat{v} \rangle_{I-R}$ includes a constituent that is *even* in \mathbf{q} [20] – which we define as $\langle \delta \hat{v}_{\parallel} \rangle_{I-R} \equiv \frac{1}{2} [(\hat{v}_{\parallel}(\mathbf{q}))_{I-R} + (\hat{v}_{\parallel}(-\mathbf{q}))_{I-R}]$ – due to the combined action of interference and spin-dependent scattering at the interface, as long as the magnetization \mathbf{m} is *not* perpendicular to the x - y plane.

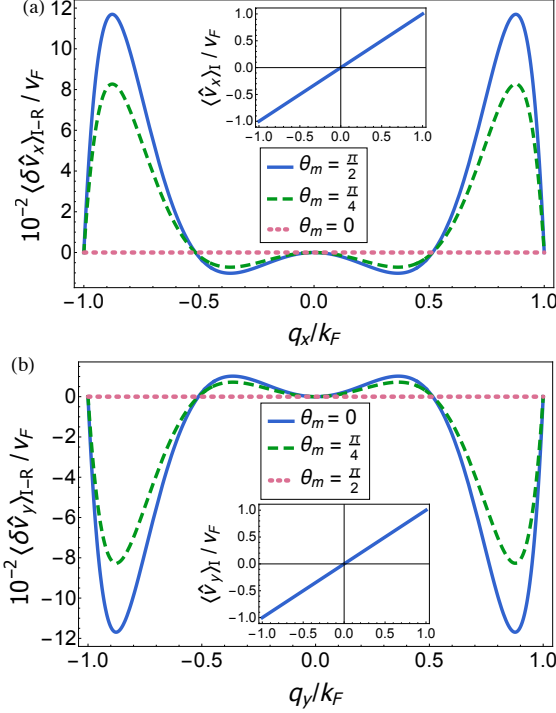


FIG. 2. The even part of the spatial average of $\langle \hat{v}_{\parallel}(\mathbf{q}) \rangle_{I-R}$, given by $\langle \delta \hat{v}_{\parallel} \rangle_{I-R} = \frac{1}{2} [\langle \hat{v}_{\parallel}(\mathbf{q}) \rangle_{I-R} + \langle \hat{v}_{\parallel}(-\mathbf{q}) \rangle_{I-R}]$, as a function of in-plane momentum for three different values of θ_m . (a) Plots of $\langle \delta \hat{v}_x \rangle_{I-R}$ (main) and $\langle \hat{v}_x \rangle_I$ (inset) as functions of q_x at $q_y = 0$. (b) Plots of $\langle \delta \hat{v}_y \rangle_{I-R}$ (main) and $\langle \hat{v}_y \rangle_I$ (inset) as functions of q_y at $q_x = 0$.

Furthermore, $\langle \hat{v} \rangle_I$ and $\langle \hat{v} \rangle_R$ are inert to the rotation of the magnetization \mathbf{m} , but $\langle \hat{v}_{\parallel} \rangle_{I-R}$ is *not*. In fact, the latter is exquisitely sensitive to the variation in the angle formed by \mathbf{m} and \mathbf{q} , with $\langle \delta \hat{v}_x \rangle_{I-R}$ and $\langle \delta \hat{v}_y \rangle_{I-R}$ exhibiting different angular dependences. It is these distinctive features of the interference velocity that give rise to the QUMR, as we will evaluate below.

QUMR.—Having derived the spin-averaged velocity $\langle \hat{v}_{\parallel} \rangle$, the in-plane charge current density can be calculated via $\mathbf{j} = \frac{-e}{(2\pi)^3} \int d^3\mathbf{k} \langle \hat{v}_{\parallel}(\mathbf{k}) \rangle \delta f(\mathbf{k})$, where $\delta f(\mathbf{k})$ is the deviation of the distribution function from equilibrium. When an electric field \mathbf{E} is applied in the x - y plane, the electron distribution in the \mathbf{k} -space is shifted by an amount $\delta\mathbf{k} = -e\tau\mathbf{E}/\hbar$, *i.e.*, $f_0(\mathbf{k}) \rightarrow f_0(\mathbf{k} - \delta\mathbf{k})$.

To capture the nonlinear charge transport, it suffices to expand the distribution up to the second-order in \mathbf{E} , with the deviation expressed by $\delta f = \delta f^{(1)} + \delta f^{(2)} + \mathcal{O}(\mathbf{E}^3)$. While the first-order term, $\delta f^{(1)} = E_i \left(\frac{\tau e}{\hbar} \right) \frac{\partial f_0}{\partial k_i}$, with i summed over x and y , is responsible for the usual linear transport, the nonlinear charge transport – and the consequent UMR – are germinated from the second-order distribution $\delta f^{(2)} = E_i E_j \left(\frac{\tau e}{\hbar} \right)^2 \frac{\partial^2 f_0}{\partial k_i \partial k_j}$, which can be approximated, at low temperatures (as compared to

the Fermi temperature), as

$$\delta f^{(2)} \simeq -\frac{(\tau e)^2}{m_e^*} E_i E_j \left(\delta_{ij} + q_i \frac{\partial}{\partial q_j} \right) \delta(\epsilon_k - \epsilon_F), \quad (8)$$

wherein δ_{ij} denotes the Kronecker delta and $\epsilon_k = \hbar^2 (q^2 + k_z^2) / 2m_e^*$ is the energy dispersion of the 3D electron gas in the NM layer.

The second-order electron distribution $\delta f^{(2)}$ is an even function of \mathbf{q} , as indicated by Eq. (8). It follows that the corresponding nonlinear charge current, $\mathbf{j}^{(2)} \sim \int d^3\mathbf{k} \langle \hat{v}_{\parallel} \rangle \delta f^{(2)}$, would simply vanish, should the velocity $\langle \hat{v}_{\parallel} \rangle$ be odd in \mathbf{q} . But this is not the case with the interference velocity $\langle \delta \hat{v}_{\parallel} \rangle_{I-R}$, which in general carries a component that is even in \mathbf{q} . In other words, it is the interference velocity that leads to the nonlinear charge current density of the form

$$j_i^{(2)}(z; \mathbf{m}) = \sigma_{ijk}(z; \mathbf{m}) E_j E_k, \quad (9)$$

with the nonlinear response function (a rank-three tensor)

$$\sigma_{ijk} = \frac{\tau^2 e^3}{(2\pi)^3 \hbar^2} \int d^2\mathbf{q} \langle \hat{v}_i(\mathbf{q}, k_{z,F}) \rangle_{I-R} \left(\frac{\delta_{jk}}{k_{z,F}} + \frac{q_j q_k}{k_{z,F}^3} \right). \quad (10)$$

Here, $k_{z,F} = \sqrt{k_F^2 - q^2}$ with $k_F (= \sqrt{2m_e^* \epsilon_F / \hbar^2})$ the Fermi wavevector, and the integration over k_z , which has been carried out in Eq. (10), can be limited to occupied states with $k_z > 0$, since only electrons moving toward the Rashba interface would acquire an interference velocity and contribute to σ_{ijk} .

In Eq. (9), we have explicitly noted the dependence of σ_{ijk} on the spatial coordinate z and the magnetization \mathbf{m} , a property inherited from the interference velocity [see Eq. (7)]. Without loss of generality, let us fix \mathbf{E} to the \mathbf{x} -direction, so that we are only concerned with two tensor elements: σ_{xxx} and σ_{yxx} , governing the nonlinear charge transport in the longitudinal and transverse directions, respectively.

One can show that σ_{xxx} must vanish when \mathbf{m} is parallel to the x -axis, whereas σ_{yxx} has to be zero when \mathbf{m} is parallel to the y -axis (which is perpendicular to \mathbf{E}). These results can be understood intuitively by the following symmetry analysis. When \mathbf{m} is in the \mathbf{x} or $-\mathbf{x}$ direction, the system is invariant under the mirror reflection in the yz plane (*i.e.*, $\mathcal{M}_x : x \rightarrow -x$) – and so are σ_{ijk} – whereby the nonlinear current density and electric field follow the change $\{E_x; j_x^{(2)}, j_y^{(2)}\} \rightarrow \{-E_x; -j_x^{(2)}, j_y^{(2)}\}$. As a result, the nonlinear response relation must satisfy $j_x^{(2)} = \sigma_{xxx} E_x E_x = -j_x^{(2)}$, so $\sigma_{xxx}(\mathbf{m} = \pm\mathbf{x}) = 0$. Similarly, when \mathbf{m} is parallel to the y -axis, the mirror reflection in the xz plane (*i.e.*, $\mathcal{M}_y : y \rightarrow -y$) leads to $j_y^{(2)} = \sigma_{yxx} E_x E_x = -j_y^{(2)}$, *i.e.*, $\sigma_{yxx}(\mathbf{m} = \pm\mathbf{y}) = 0$.

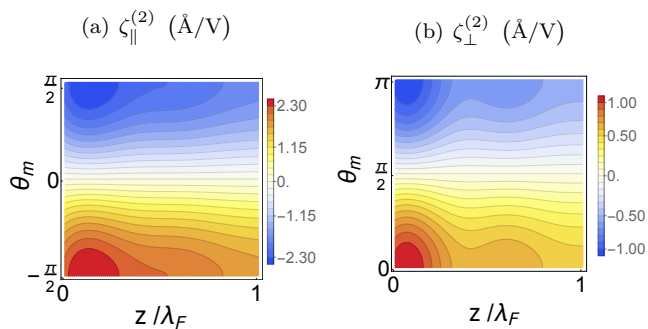


FIG. 3. Plots of the (a) longitudinal and (b) transverse QUMRs as functions of z/λ_F and θ_m , where $\lambda_F = 2\pi/k_F$ is the Fermi wavelength. Note the antisymmetry of the longitudinal QUMR about the $\theta_m = 0$ line, showing an angular dependence of $\mathbf{E} \times \mathbf{m}$, and that of the transverse QUMR about the $\theta_m = \pi/2$ line, showing a different angular dependence of $\mathbf{E} \cdot \mathbf{m}$. Parameters used: $\xi_{\text{ex}}/k_F = 0.2$ [22], $\eta_R = 0.2$ [23–26], $m_e^* = 1.8 \times 10^{-30}$ kg, $\epsilon_F = 5.0$ eV, $V_b = 8.0$ eV, and $\tau = 10^{-14}$ s.

For a quantitative characterization of the nonlinear transport effect, it is helpful to introduce two new quantities – the UMR coefficients $\zeta_{\parallel}^{(2)}$ and $\zeta_{\perp}^{(2)}$:

$$\zeta_{\parallel}^{(2)} \equiv \frac{\sigma_{xx}(E_x) - \sigma_{xx}(-E_x)}{\sigma_D E_x} \simeq -\frac{2\sigma_{xxx}}{\sigma_D}, \quad (11a)$$

$$\zeta_{\perp}^{(2)} \equiv \frac{\sigma_{yx}(E_x) - \sigma_{yx}(-E_x)}{\sigma_D E_x} \simeq -\frac{2\sigma_{yxx}}{\sigma_D}, \quad (11b)$$

which characterize, respectively, the longitudinal and transverse QUMRs. Here $\sigma_{ij} = j_i/E_j$ denote the linear conductivity tensors, and σ_D is the Drude conductivity of the NM layer. It is worth noting that the UMR coefficients, $\zeta_{\parallel}^{(2)}$ and $\zeta_{\perp}^{(2)}$, are so defined that both of them are independent of the external electric field. Physically, the inverse of the UMR coefficient – which has the dimension of an electric field – sets the scale of the applied electric field for which the nonlinear conductivity becomes comparable to the linear conductivity.

In Fig. 3, we plot $\zeta_{\parallel}^{(2)}$ and $\zeta_{\perp}^{(2)}$ as functions of z and θ_m (the angle between the in-plane magnetization and the electric field). Note that the longitudinal and transverse QUMRs exhibit distinctly different angular dependences, with $\zeta_{\parallel}^{(2)} \sim \sin\theta_m$ and $\zeta_{\perp}^{(2)} \sim \cos\theta_m$, consistent with the vectorial form of the nonlinear current density [21] presented in Eq. (1). The spatial variations in $\zeta_{\parallel}^{(2)}$ and $\zeta_{\perp}^{(2)}$, on the other hand, occur over the same length scale – the Fermi wavelength λ_F , reflecting the quantum nature of the nonlinear transport effect.

Materials considerations. – The most promising materials systems to observe the QUMR effect are probably bilayers consisting of a heavy-metal and a FI, such as Au|YIG (Yttrium iron garnet) and β -Ta|YIG. These systems possess a magnetic interface with sizable Rashba

SOC and exchange interaction – two essential ingredients for generating QUMR. And, qualitatively, the larger the interfacial interactions, the stronger the QUMR, since the leading-order contribution to the QUMR increases linearly with the strengths of the interactions characterized by α_R and J_{ex} [27].

In principle, QUMR may also arise in metallic bilayers comprising a heavy-metal and a ferromagnetic-metal, but it would be accompanied by two other nonlinear effects taking place in the metallic ferromagnetic layer. One main competitor is the spin-Hall UMR [11, 16, 18], arising from the spin accumulation built in the ferromagnetic-metal layer due to spin-current injection driven by the spin Hall effect [28–30] in the heavy-metal layer. For a typical metallic bilayer, such as Pt|Co, the corresponding UMR coefficient is about $\zeta^{(2)} \sim 1$ Å/V, about the same order of magnitude as the predicted QUMR in a typical NM|FI bilayer. The other nonlinear effect that may intertwine with the QUMR is the anomalous Nernst effect [31]: the Joule heating may induce a vertical temperature gradient $\nabla T (\propto \mathbf{E}^2)$ across the ferromagnetic-metal layer, which would in turn give rise to a nonlinear current in the direction of $\mathbf{m} \times \nabla T$. The absence of these competing effects in a FI makes NM|FI bilayers a better platform for observing the QUMR effect.

Closing remarks. – In conclusion, we have explored electron quantum transport in the nonlinear response regime, and predicted a QUMR effect in NM|FI bilayers, which originates from the interference between electron waves approaching and reflecting off a magnetic interface with Rashba SOC.

Several appealing properties of the QUMR have been identified, enabling both electric and magnetic control of the nonlinear magnetotransport effect. In contrast to the well-known linear magnetoresistance due to WL or WAL, which is independent of the external electric field, the emergence of the QUMR effect entails variations in both longitudinal and transverse resistances whenever the direction of the electric field is reversed. Moreover, the QUMR is also sensitive to the orientation of magnetization of the FI layer, as the phase difference between the scattering waves can be tuned by the magnetization through its coupling with the spin angular momenta of conduction electrons in the NM layer.

We envision that this work will stimulate further theoretical and experimental studies of nonlinear quantum magnetotransport in various materials systems and nanostructures, and potentially open new avenues for developing future quantum spintronic devices.

Acknowledgment. – The authors are grateful to Giovanni Vignale for helpful comments and for a critical reading of the manuscript. This work was supported by the College of Arts and Sciences, Case Western Reserve University.

-
- * shulei.zhang@case.edu
- [1] P. W. Anderson, *Phys. Rev.*, **109**, 1492 (1958).
- [2] E. Abrahams, P. W. Anderson, D. C. Licciardello, and T. V. Ramakrishnan, *Phys. Rev. Lett.*, **42**, 673 (1979).
- [3] G. Bergmann, *Phys. Rep.*, **107**, 1 (1984).
- [4] R. A. Webb, S. Washburn, C. P. Umbach, and R. B. Laibowitz, *Phys. Rev. Lett.*, **54**, 2696 (1985).
- [5] A. Bachtold, C. Strunk, J.-P. Salvetat, J.-M. Bonard, L. Forró, T. Nussbaumer, and C. Schönenberger, *Nature*, **397**, 673 (1999).
- [6] H. Peng, K. Lai, D. Kong, S. Meister, Y. Chen, X.-L. Qi, S.-C. Zhang, Z.-X. Shen, and Y. Cui, *Nat. Mater.*, **9**, 225 (2010).
- [7] B. Spivak, S. V. Kravchenko, S. A. Kivelson, and X. P. A. Gao, *Rev. Mod. Phys.*, **82**, 1743 (2010).
- [8] A. M. Whiticar, A. Fornieri, E. C. T. O’Farrell, A. C. C. Drachmann, T. Wang, C. Thomas, S. Gronin, R. Kallagher, G. C. Gardner, M. J. Manfra, C. M. Marcus, and F. Nichele, *Nat. Commun.*, **11**, 3212 (2020).
- [9] B. L. Altshuler, D. Khmel’nitzkii, A. I. Larkin, and P. A. Lee, *Phys. Rev. B*, **22**, 5142 (1980).
- [10] S. Hikami, A. I. Larkin, and Y. Nagaoka, *Prog. Theor. Phys.*, **63**, 707 (1980).
- [11] C. O. Avci, K. Garello, A. Ghosh, M. Gabureac, S. F. Alvarado, and P. Gambardella, *Nat. Phys.*, **11**, 570 (2015).
- [12] K. Olejník, V. Novák, J. Wunderlich, and T. Jungwirth, *Phys. Rev. B*, **91**, 180402 (2015).
- [13] K. Yasuda, A. Tsukazaki, R. Yoshimi, K. S. Takahashi, M. Kawasaki, and Y. Tokura, *Phys. Rev. Lett.*, **117**, 127202 (2016).
- [14] Y. Lv, J. Kally, D. Zhang, J. S. Lee, M. Jamali, N. Samarth, and J.-P. Wang, *Nat. Commun.*, **9**, 111 (2018).
- [15] T. Guillet, A. Marty, C. Vergnaud, M. Jamet, C. Zucchetti, G. Isella, Q. Barbedienne, H. Jaffrès, N. Reyren, J. M. George, and A. Fert, *Phys. Rev. B*, **103**, 064411 (2021).
- [16] S. S.-L. Zhang and G. Vignale, *Phys. Rev. B*, **94**, 140411 (2016).
- [17] S. Langenfeld, V. Tshitoyan, Z. Fang, A. Wells, T. A. Moore, and A. J. Ferguson, *Appl. Phys. Lett.*, **108**, 192402 (2016).
- [18] C. O. Avci, J. Mendil, G. S. D. Beach, and P. Gambardella, *Phys. Rev. Lett.*, **121**, 087207 (2018).
- [19] See Sec. A in the Supplemental Material for detailed derivation of the scattering amplitude matrix.
- [20] The interference velocity also has a component that is odd in \mathbf{q} , which contributes to an anisotropic magnetoresistance – in linear response to the applied electric field – with an angular dependence similar to the spin-Hall magnetoresistance [32–34].
- [21] See Sec. B in the Supplemental Material for detailed derivation of the vectorial form of the nonlinear charge current density.
- [22] Y. Kajiwara, K. Harii, S. Takahashi, J. Ohe, K. Uchida, M. Mizuguchi, H. Umezawa, H. Kawai, K. Ando, K. Takanashi, S. Maekawa, and E. Saitoh, *Nature (London)*, **464**, 262 (2010).
- [23] I. Mihai Miron, G. Gaudin, S. Auffret, B. Rodmacq, A. Schuhl, S. Pizzini, J. Vogel, and P. Gambardella, *Nat. Mater.*, **9**, 230 (2010).
- [24] J.-H. Park, C. H. Kim, H.-W. Lee, and J. H. Han, *Phys. Rev. B*, **87**, 041301 (2013).
- [25] I. V. Tokatly, E. E. Krasovskii, and G. Vignale, *Phys. Rev. B*, **91**, 035403 (2015).
- [26] S. Grytsyuk, A. Belabbes, P. M. Haney, H.-W. Lee, K.-J. Lee, M. D. Stiles, U. Schwingenschlögl, and A. Manchon, *Phys. Rev. B*, **93**, 174421 (2016).
- [27] See Sec. B in the Supplemental Material for the plots of the (spatially averaged) UMR coefficients, *i.e.*, $\zeta_{\parallel}^{(2)}$ and $\zeta_{\perp}^{(2)}$, as functions of α_R and J_{ex} .
- [28] M. I. Dyakonov and V. I. Perel, *Phys. Lett. A*, **35**, 459 (1971).
- [29] J. E. Hirsch, *Phys. Rev. Lett.*, **83**, 1834 (1999).
- [30] S. Zhang, *Phys. Rev. Lett.*, **85**, 393 (2000).
- [31] S. Y. Huang, W. G. Wang, S. F. Lee, J. Kwo, and C. L. Chien, *Phys. Rev. Lett.*, **107**, 216604 (2011).
- [32] H. Nakayama *et al.*, *Phys. Rev. Lett.*, **110**, 206601 (2013).
- [33] V. L. Grigoryan, W. Guo, G. E. W. Bauer, and J. Xiao, *Phys. Rev. B*, **90**, 161412 (2014).
- [34] S. S.-L. Zhang, G. Vignale, and S. Zhang, *Phys. Rev. B*, **92**, 024412 (2015).

Supplemental Material for “Quantum Unidirectional Magnetoresistance”

M. Mehraeen,^{*} Pengtao Shen, and Steven S.-L. Zhang[†]
Department of Physics, Case Western Reserve University, Cleveland, OH 44106, USA
(Dated: September 1, 2021)

A. SCATTERING AMPLITUDE MATRICES

Consider a 3D electron gas in the scattering potential [S1, S2]

$$\hat{V}_s(z) = \frac{\alpha_R}{\hbar} \delta(z) \hat{\sigma} \cdot (\hat{\mathbf{p}} \times \mathbf{z}) - J_{ex} \delta(z) \hat{\sigma} \cdot \mathbf{m} + V_b \Theta(-z), \quad (\text{S.1})$$

where α_R and J_{ex} are the coefficients of the interfacial Rashba spin-orbit coupling (SOC) and exchange interaction, respectively, and V_b is the height of the energy barrier, which is greater than the Fermi energy of electrons in the NM layer.

The general scattering state is given as

$$\psi_{\text{scat.}} = \begin{cases} e^{i\mathbf{q}\cdot\rho} \left(e^{-ik_z z} + e^{ik_z z} \hat{R} \right) \chi, & z > 0 \quad (\text{NM Layer}) \\ e^{i\mathbf{q}\cdot\rho} e^{\kappa z} \hat{T} \chi, & z < 0 \quad (\text{FI Layer}) \end{cases}, \quad (\text{S.2})$$

where $\mathbf{q} [= (k_x, k_y)]$ and $\rho [= (x, y)]$ are the wave- and position-vectors in the x - y plane, wherein the system is translationally invariant and allows propagation of plane waves, k_z is the z -component of the wavevector of the propagating wave in the NM layer, and $\kappa^{-1} [= (2m_e^* V_b / \hbar^2 - k_z^2)^{-1/2}]$ characterizes the decay length of the evanescent wave in the FI layer. \hat{R} and \hat{T} are 2×2 matrices in spin space, which describe, respectively, the spin-dependent reflection and transmission amplitudes, and the spinors χ can be taken as an arbitrary superposition of the eigenspinors that satisfy $\hat{\sigma} \cdot \mathbf{m} \chi^\pm = \pm \chi^\pm$.

The wavefunction obeys the following boundary conditions at the Rashba interface

$$\psi_{\text{scat.}}(\rho, 0^+) = \psi_{\text{scat.}}(\rho, 0^-), \quad (\text{S.3a})$$

$$\frac{d}{dz} \psi_{\text{scat.}}(\rho, 0^+) - \frac{d}{dz} \psi_{\text{scat.}}(\rho, 0^-) = \hat{\sigma} \cdot \mathbf{Q}_q \psi_{\text{scat.}}(\rho, 0), \quad (\text{S.3b})$$

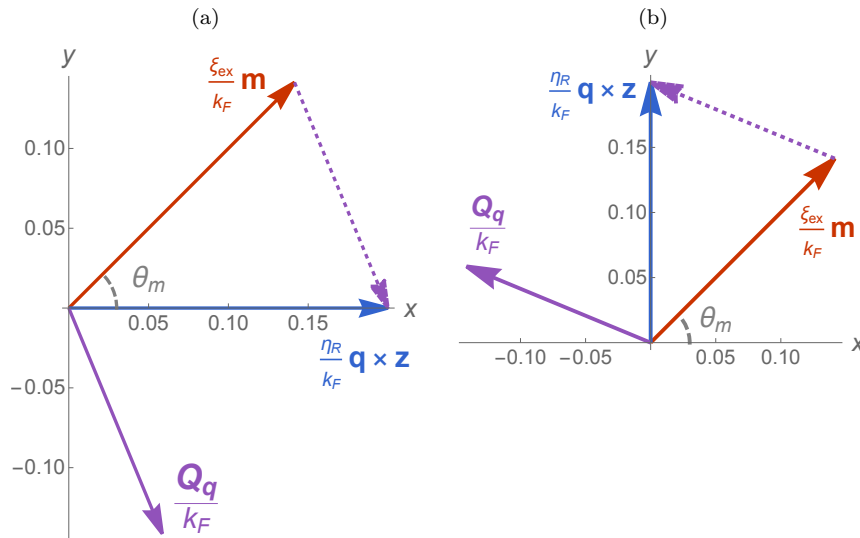


FIG. S.1. Plots of the dimensionless vectors $\eta_R \mathbf{q} \times \mathbf{z} / k_F$, $\xi_{ex} \mathbf{m} / k_F$ and $\mathbf{Q}_q / k_F = (\eta_R \mathbf{q} \times \mathbf{z} - \xi_{ex} \mathbf{m}) / k_F$ for the unit vectors (a) $\mathbf{q} \times \mathbf{z} / k_F = \mathbf{x}$ and (b) $\mathbf{q} \times \mathbf{z} / k_F = \mathbf{y}$. Parameters used: $\eta_R = \xi_{ex} / k_F = 0.2$ and $\theta_m = \cos^{-1}(\mathbf{m} \cdot \mathbf{x}) = \pi/4$.

where $\mathbf{Q}_{\mathbf{q}} = \eta_R \mathbf{q} \times \mathbf{z} - \xi_{ex} \mathbf{m}$ –as shown in Fig. S.1– with $\eta_R \equiv 2m_e^* \alpha_R / \hbar^2$ a dimensionless constant characterizing the strength of the interfacial Rashba SOC and $\xi_{ex} \equiv 2m_e^* J_{ex} / \hbar^2$ the rescaled exchange interaction. Eliminating χ and $e^{i\mathbf{q}\cdot\rho}$ from Eqs. (S.3a) and (S.3b), we obtain a set of equations for the scattering amplitude matrices:

$$1 + \hat{R} = \hat{T}, \quad (\text{S.4a})$$

$$-ik_z (1 - \hat{R}) - \kappa \hat{T} = \hat{\sigma} \cdot \mathbf{Q}_{\mathbf{q}} \hat{T}. \quad (\text{S.4b})$$

Solving the set of equations, one can obtain the general expression of the reflection amplitude matrix as follows

$$\hat{R} = \frac{\mathbf{Q}_{\mathbf{q}}^2 - (\kappa^2 + k_z^2) + 2ik_z \hat{\sigma} \cdot \mathbf{Q}_{\mathbf{q}}}{(\kappa - ik_z)^2 - \mathbf{Q}_{\mathbf{q}}^2}, \quad (\text{S.5})$$

which is Eq. (4) presented in the main text.

B. NONLINEAR CHARGE CURRENT DENSITY

We start with the form of the nonlinear conductivity tensor given by Eq. (10) in the main text

$$\sigma_{ijk}(z) = \frac{\tau^2 e^3}{(2\pi)^3 \hbar^2} \int d\mathbf{q} \langle \hat{v}_i(\mathbf{q}, k_{z,F}) \rangle_{I-R} \left(\frac{\delta_{jk}}{k_{z,F}} + \frac{q_j q_k}{k_{z,F}^3} \right), \quad (\text{S.6})$$

where $k_{z,F} = \sqrt{k_F^2 - q^2}$ and

$$\langle \hat{v}_i(\mathbf{q}, k_{z,F}) \rangle_{I-R} = \frac{2\hbar q_i}{m_e^*} \text{Re} \left(e^{2ik_{z,F}z} \text{Tr} \hat{R} \right), \quad (\text{S.7})$$

Note that Eq. (S.7) is equivalent to Eq. (7) in the main text.

In general, σ_{ijk} will have 8 components in two dimensions. However, we note from Eq. (S.6) that $\sigma_{ijk} = \sigma_{ikj}$, as required by intrinsic permutation symmetry, which brings the number down to 6. We integrate out the polar angle in momentum space and take the spatial average. Furthermore, we keep terms up to $\mathcal{O}(\eta_R, \xi_{ex})$, which is a good

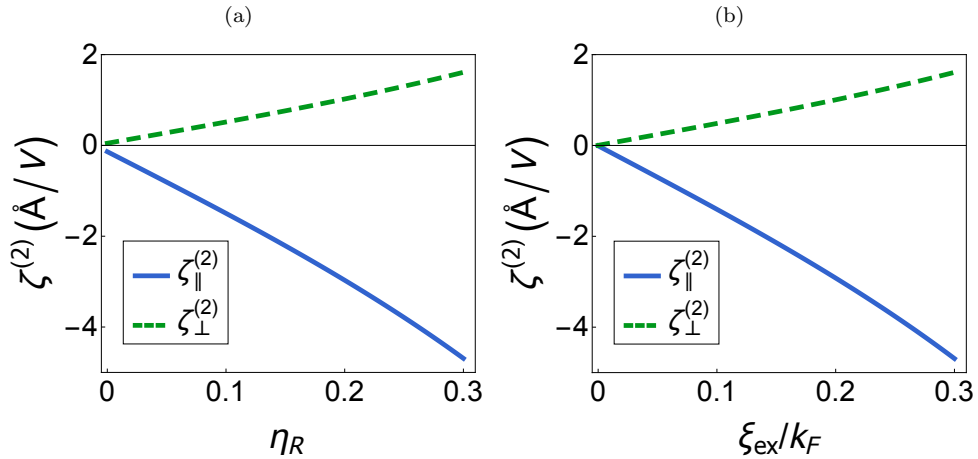


FIG. S.2. Dependences of the UMR coefficients on the Rashba SOC and exchange constants, which, to a good approximation, remain linear in the region considered. Plots of $\zeta_{\parallel}^{(2)}$ and $\zeta_{\perp}^{(2)}$ as functions of (a) η_R at $\xi_{ex}/k_F = 0.2$ and (b) ξ_{ex}/k_F at $\eta_R = 0.2$. Parameters used: $m_e^* = 1.8 \times 10^{-30}$ kg, $\epsilon_F = 5.0$ eV, $V_b = 8.0$ eV, and $\tau = 10^{-14}$ s.

approximation, as shown in Fig. S.2. Then, the nonlinear conductivities read

$$\bar{\sigma}_{xxx} \simeq \frac{e^3 \eta_R \xi_{ex} \tau^2}{4\pi^2 \hbar m_e^* d_N} m_y \int_0^{k_F} dq (3q^5 + 4k_{z,F}^2 q^3) \left[\frac{2\kappa_F (\kappa_F^2 - 3k_{z,F}^2) \sin^2(d_N k_{z,F}) - k_{z,F} (k_{z,F}^2 - 3\kappa_F^2) \sin(2d_N k_{z,F})}{k_{z,F}^3 (\kappa_F^2 + k_{z,F}^2)^3} \right], \quad (\text{S.8a})$$

$$\bar{\sigma}_{xxy} \simeq -\frac{e^3 \eta_R \xi_{ex} \tau^2}{4\pi^2 \hbar m_e^* d_N} m_x \int_0^{k_F} dq q^5 \left[\frac{2\kappa_F (\kappa_F^2 - 3k_{z,F}^2) \sin^2(d_N k_{z,F}) - k_{z,F} (k_{z,F}^2 - 3\kappa_F^2) \sin(2d_N k_{z,F})}{k_{z,F}^3 (\kappa_F^2 + k_{z,F}^2)^3} \right], \quad (\text{S.8b})$$

$$\bar{\sigma}_{xyy} \simeq \frac{e^3 \eta_R \xi_{ex} \tau^2}{4\pi^2 \hbar m_e^* d_N} m_y \int_0^{k_F} dq (q^5 + 4k_{z,F}^2 q^3) \left[\frac{2\kappa_F (\kappa_F^2 - 3k_{z,F}^2) \sin^2(d_N k_{z,F}) - k_{z,F} (k_{z,F}^2 - 3\kappa_F^2) \sin(2d_N k_{z,F})}{k_{z,F}^3 (\kappa_F^2 + k_{z,F}^2)^3} \right], \quad (\text{S.8c})$$

$$\bar{\sigma}_{yxx} \simeq -\frac{e^3 \eta_R \xi_{ex} \tau^2}{4\pi^2 \hbar m_e^* d_N} m_x \int_0^{k_F} dq (q^5 + 4k_{z,F}^2 q^3) \left[\frac{2\kappa_F (\kappa_F^2 - 3k_{z,F}^2) \sin^2(d_N k_{z,F}) - k_{z,F} (k_{z,F}^2 - 3\kappa_F^2) \sin(2d_N k_{z,F})}{k_{z,F}^3 (\kappa_F^2 + k_{z,F}^2)^3} \right], \quad (\text{S.8d})$$

$$\bar{\sigma}_{yyx} \simeq \frac{e^3 \eta_R \xi_{ex} \tau^2}{4\pi^2 \hbar m_e^* d_N} m_y \int_0^{k_F} dq q^5 \left[\frac{2\kappa_F (\kappa_F^2 - 3k_{z,F}^2) \sin^2(d_N k_{z,F}) - k_{z,F} (k_{z,F}^2 - 3\kappa_F^2) \sin(2d_N k_{z,F})}{k_{z,F}^3 (\kappa_F^2 + k_{z,F}^2)^3} \right], \quad (\text{S.8e})$$

$$\bar{\sigma}_{yyy} \simeq -\frac{e^3 \eta_R \xi_{ex} \tau^2}{4\pi^2 \hbar m_e^* d_N} m_x \int_0^{k_F} dq (3q^5 + 4k_{z,F}^2 q^3) \left[\frac{2\kappa_F (\kappa_F^2 - 3k_{z,F}^2) \sin^2(d_N k_{z,F}) - k_{z,F} (k_{z,F}^2 - 3\kappa_F^2) \sin(2d_N k_{z,F})}{k_{z,F}^3 (\kappa_F^2 + k_{z,F}^2)^3} \right], \quad (\text{S.8f})$$

where $\kappa_F = (2m_e^* V_b / \hbar^2 - k_{z,F}^2)^{1/2}$ and d_N is the thickness of the NM layer. Introducing the definitions

$$\sigma_{\parallel}^{(2)} = \frac{\sigma_{xxx}}{m_y} = -\frac{\sigma_{yyy}}{m_x}, \quad (\text{S.9a})$$

$$\sigma_{\perp}^{(2)} = \frac{\sigma_{yxx}}{m_x} = -\frac{\sigma_{xyy}}{m_y}, \quad (\text{S.9b})$$

and noting the following relations among the conductivity tensor components

$$\sigma_{xxx} - 2\sigma_{yxy} - \sigma_{xyy} = 0, \quad (\text{S.10a})$$

$$\sigma_{yyy} - 2\sigma_{xyx} - \sigma_{yxx} = 0, \quad (\text{S.10b})$$

we find that the nonlinear charge current density takes the concise vectorial form

$$\mathbf{j}^{(2)} = \sigma_{\parallel}^{(2)} \mathbf{z} \cdot \mathbf{E} \times \mathbf{m} \mathbf{E} + \sigma_{\perp}^{(2)} \mathbf{E} \cdot \mathbf{m} \mathbf{z} \times \mathbf{E}, \quad (\text{S.11})$$

which is Eq. (1) presented in the main text.

* mxm1289@case.edu

† shulei.zhang@case.edu

[S1] P. M. Haney, H.-W. Lee, K.-J. Lee, A. Manchon, and M. D. Stiles, *Phys. Rev. B*, **87**, 174411 (2013).

[S2] I. V. Tokatly, E. E. Krasovskii, and G. Vignale, *Phys. Rev. B*, **91**, 035403 (2015).